



Charm-quark pole mass from HERA Combined and LHCb charm production data

A. Vafaei 

*Department of Physics, Ferdowsi University of Mashhad, P.O.Box 1436, Mashhad, Iran and
School of Particles and Accelerators,
Institute for Research in Fundamental Sciences (IPM), P.O.Box 19395-5531, Tehran, Iran*

K. Javidan 

Department of Physics, Ferdowsi University of Mashhad, P.O.Box 1436, Mashhad, Iran

S. Atashbar Tehrani 

*School of Particles and Accelerators,
Institute for Research in Fundamental Sciences (IPM), P.O.Box 19395-5531, Tehran, Iran*

Abstract

One of the most popular definition for the charm-quark mass is the charm-quark pole mass m_c^{pole} . In this contribution, we extract the charm-quark pole mass through perturbative Quantum Chromo Dynamics (pQCD) analysis up to the next-to-next-to-leading order (NNLO) corrections from HERA Combined and LHCb charm production recent data sets. Then, we investigate for the first time the charm-quark pole mass m_c^{pole} pure impact, as an extra pQCD parameter on the proton Parton Distribution Functions (PDFs) at the NNLO corrections.

I. INTRODUCTION

The HERA machine as a powerful electron-proton collider study simultaneously neutral current (NC) and charged current (CC) $e^\pm p$ collisions and their electroweak unification process. On the other hand, the LHCb detector studies the charm-quark production at the Large Hadron Collider (LHC) in pp reactions at $\sqrt{s} = 7$ TeV.

At the pQCD level the internal structure of the proton is probed by the experiments known as deep inelastic scattering (DIS) measurements. The DIS experiments serve the central data to determine the nucleon structure in terms of parton distribution functions. Contributions from all active quarks and anti quarks are included by the inclusive neutral NC and CC deep inelastic $e^\pm p$ scattering cross sections.

At the DIS measurement level the ratio of the virtual photon couplings corresponding to a heavy quark $Q_h, h = b, c$ are approximated by $f(h) \sim \frac{Q_h^2}{\sum Q_q^2}$, where $Q_h = \frac{1}{3}, \frac{2}{3}$ are the b -quark and c -quark electric charges, respectively and Q_q with $q = u, d, s, c, b$ represent the kinematically accessible quark flavors. Accordingly, $f(c) \sim \frac{Q_c^2}{Q_d^2 + Q_u^2 + Q_s^2 + Q_c^2 + Q_b^2} = \frac{4}{11} \simeq 0.36$ for the c -quark and this means that more than one third (or approximately 36 percent) of the cross sections come from charm quarks in the final state. This significant contribution of c -quark at the HERA events is our main motivation to determine the charm-quark pole mass based on the very recently charm production cross section H1-ZEUS combined (HCC) [1], LHCb [2] and HCC+LHCb charm production cross section data sets. Then, we investigate the pure impact of the charm-quark pole mass m_c^{pole} as an extra free parameter of the pQCD Lagrangian on the uncertainty bands of gluon distribution and some of its ratios at the NNLO corrections.

In this NNLO pQCD analysis we make several fits to exactly separate the role and influence of charm-quark pole mass m_c^{pole} from other phenomenological parameters on the uncertainty bands of PDFs and fit-quality, based on the HCC, LHCb and HCC+LHCb data sets within the pQCD framework.

From the pQCD point of view, DIS measurements depend on the various phenomenological input data and knowledge of the PDFs [3–7]. For this reason in addition of charm production cross section from the HERA combined data, the full five LHCb charm production cross section data sets at $\sqrt{s} = 7$ TeV are included to show the sensitivity of the gluon distribution and some of related ratios at low values of x , where x is the fraction of proton

momentum carried by a parton. Since this kinematic range does not currently covered by other data set, inclusion of the LHCb charm production data at $\sqrt{s} = 7$ TeV dramatically improve the gluon distribution uncertainties and fit quality [8–14].

The outline of this paper is as follows. In Sec. (II) we describe the theoretical framework of our study and discuss about the inclusive differential cross section of charm-quark production. We introduce the charm-quark mass in the pQCD approach in Sec. (III). In Sec. (IV), we describe the data set and our methodology. The results are presented in Sec. (V) and then, we conclude with a summary in Sec. (VI).

II. CHARM-QUARK PRODUCTION

The NC and CC deep inelastic $e^\pm p$ scattering at the centre-of-mass energies up to $\sqrt{s} \simeq 320$ GeV are expressed in terms of the proton generalized structure functions:

$$\sigma_{r,NC}^\pm = \frac{d^2\sigma_{NC}^{e^\pm p}}{dx dQ^2} \frac{Q^4 x}{2\pi\alpha^2 Y_+} = \tilde{F}_2 \mp \frac{Y_-}{Y_+} x \tilde{F}_3 - \frac{y^2}{Y_+} \tilde{F}_L, \quad (1)$$

$$\sigma_{r,CC}^\pm = \frac{2\pi x}{G_F^2} \left[\frac{M_W^2 + Q^2}{M_W^2} \right]^2 \frac{d^2\sigma_{CC}^{e^\pm p}}{dx dQ^2} = \frac{Y_+}{2} W_2^\pm \mp \frac{Y_-}{2} x W_3^\pm - \frac{y^2}{2} W_L^\pm, \quad (2)$$

where x is the Bjorken variable, y is the inelasticity, Q^2 is the negative of four-momentum-transfer squared, $Y_\pm = 1 \pm (1-y)^2$, α is the fine-structure constant which is defined at zero momentum transfer and G_F is the Fermi constant [15].

Similarly, the inclusive differential cross section of charm production in DIS is expressed in terms of the dimensionless reduced cross sections:

$$\sigma_{red}^{C\bar{C}} = \frac{d\sigma^{C\bar{C}}(e^\pm p)}{dx dQ^2} \frac{Q^4 x}{2\pi\alpha^2 Y_+} = F_2^{C\bar{C}} \mp \frac{Y_-}{Y_+} x F_3^{C\bar{C}} - \frac{y^2}{Y_+} F_L^{C\bar{C}}. \quad (3)$$

At the low-value regions of Q^2 where $Q^2 \ll M_Z^2$, the parity-violating structure function, $x F_3$ is neglected and the reduced differential cross section of charm production can be expressed by:

$$\sigma_{red}^{C\bar{C}} = \frac{d\sigma^{C\bar{C}}(e^\pm p)}{dx dQ^2} \frac{Q^4 x}{2\pi\alpha^2 Y_+} = F_2^{C\bar{C}} - \frac{y^2}{Y_+} F_L^{C\bar{C}}. \quad (4)$$

A detailed study of the inclusive deep inelastic $e^\pm p$ scattering cross sections, charm production reduced cross section, generalized structure functions for NC and CC deep inelastic $e^\pm p$ scattering and other related parameters can be found in Ref. [15].

III. CHARM-QUARK MASS IN THE PQCD APPROACH

From the theoretical point of view, the reduced charm production cross section is obtained by convolution of matrix elements with PDFs. On the other hand, PDFs are extracted from inclusive deep inelastic $e^\pm p$ scattering cross sections. Accordingly, both matrix elements and proton PDFs strictly depend on the c -quark mass [16–21].

The non-observation of free quarks is explained by the hypothesis of color confinement, which states that colored objects are always confined to color singlet states and that no objects with non-zero color charge can propagate as free particles [22–25]. Accordingly, different definitions of the charm-quark mass m_c such as the pole mass m_c^{pole} and $\overline{\text{MS}}$ running mass $m_c(\mu_r)$ are available. In pQCD, the pole mass is defined as the mass at the position of the pole in the c -quark propagator and $\overline{\text{MS}}$ running mass is the charm mass which is evaluated at the renormalization scale μ_r [26]. Each definition has own advantages and disadvantages. The pole mass m_c^{pole} is a gauge invariant quantity and is well defined in any finite order of pQCD. But it has an intrinsic uncertainty of order $\frac{\Lambda_{\text{QCD}}}{m_c}$, where $\Lambda_{\text{QCD}} \sim 0.25$ MeV is the QCD scale. The $\overline{\text{MS}}$ running mass avoid this problem and its relation with pole mass m_c^{pole} is given by

$$m_c^{\text{pole}} = m_c(m_c) \left(1 + \frac{4\alpha_s(m_c)}{3\pi} \right), \quad (5)$$

where $m_c(m_c)$ is the $\overline{\text{MS}}$ running mass evaluated at the scale $\mu_r = m_c$.

IV. DATA SET AND METHODOLOGY

In this NNLO pQCD analysis, we use three different data sets: the HERA run I and II combined NC and CC deep $e^\pm p$ scattering cross sections (HC) [27], the very recently charm production cross section H1-ZEUS combined data (HCC) [1] and the full five LHCb charm production cross section data sets at $\sqrt{s} = 7$ TeV [2].

To determine and study the pure impact of charm-quark pole mass m_c^{pole} on proton PDFs and fit-quality we make six different fits in two separate steps as follow:

At the first step we fixed the charm-quark mass to $m_c = 1.257$ GeV and make three different fits with 13 free parameters based on HCC, LHCb and HCC+LHCb charm production cross section data to investigate the pure impact of these data sets on the full HERA run I and II combined NC and CC deep $e^\pm p$ scattering data, as the central proton PDFs.

At the second step we consider the charm-quark mass m_c^{pole} as an extra free parameter of the pQCD Lagrangian and refit the above fit procedures but this time with 14 free parameters to determine simultaneously the charm-quark pole mass m_c^{pole} and pure impact of c -mass on the proton PDFs for the first time at the NNLO corrections.

Depending on the initial set-up of a QCD analysis, different approaches can be taken for treatment of the heavy quarks contribution [28–36].

To include the charm-quark contribution, we use very recently updated Fixed Flavor number scheme from Alekhin, Blumlein and Moch (FF ABM) as implemented in the xFitter package as a powerful QCD framework [37–43].

Baед on our NNLO pQCD set-up, the FF ABM scheme provides most reliable results and best fit-quality in the phase space of HCC and LHCb charm production data. In the fixed flavor number scheme heavy quarks are considered as massive at all scales but they do not considered as partons within the proton. The number of active flavors is fixed to three for c -quark and is fixed to four for b -quark. Updated variants of FFN scheme govern both charm-quark pole mass and $\overline{\text{MS}}$ running mass, however the calculations of this QCD analysis use FF ABM variant and is developed based on the charm-quark pole mass m_c^{pole} .

To parameterized the proton PDFs, we use the HERAPDF standard functional form at the initial scale of the QCD evolution $Q_0^2 = 1.9 \text{ GeV}^2$ as:

$$xf(x) = Ax^B(1-x)^C(1+Dx+Ex^2) \quad , \quad (6)$$

with 13 central free parameters and m_c as another extra free parameter. A detailed review of HERAPDF standard functional form and its related parameters has been reported in Ref. [15].

The initial set-up of this QCD analysis is based on the following additional parameters: The strong coupling constant is fixed to $\alpha_s^{\text{NNLO}}(M_Z^2) = 0.118$ [15], the strangeness suppression factor is fixed to $f_s = 0.4$ [27], the initial value of charm-quark pole mass is set to $m_c^{\text{pole}} = 1.257 \text{ GeV}$ and then varied in steps of 0.001 [37] and finally the theory type based on the DGLAP collinear evolution mode [44, 45].

V. RESULTS

Table I, shows the experiments with correlated χ^2 and χ^2_{Total} per degrees of freedom (dof) for each experiment corresponding to three different HCC, LHCb and HCC+LHCb data sets, when the charm-quark mass is fixed to $m_c = 1.257$ GeV.

Scheme	charm-quark mass is fixed to $m_c = 1.257$ GeV		
Experiment	HCC	LHCb	HCC+LHCb
HC CC e^+p [27]	56 / 39	63 / 39	63 / 39
HC CC e^-p [27]	51 / 42	50 / 42	50 / 42
HC NC e^-p [27]	218 / 159	224 / 159	224 / 159
HC NC e^+p 460 [27]	213 / 204	211 / 204	211 / 204
HC NC e^+p 575 [27]	213 / 254	210 / 254	211 / 254
HC NC e^+p 820 [27]	63 / 70	61 / 70	62 / 70
HC NC e^+p 920 [27]	427 / 377	425 / 377	426 / 377
HCC [1]	41 / 47	-	40 / 47
LHCb 7TeV Dzero [2]	-	392 / 38	389 / 38
LHCb 7TeV Dch [2]	-	117 / 37	119 / 37
LHCb 7TeV Dstar [2]	-	85 / 31	87 / 31
LHCb 7TeV Ds [2]	-	26 / 28	26 / 28
LHCb 7TeV Lambdac [2]	-	5.1 / 6	5.2 / 6
Correlated χ^2	157	157	195
$\frac{\chi^2_{Total}}{dof}$	$\frac{1410}{1179}$	$\frac{2029}{1272}$	$\frac{2078}{1319}$

Table I: Experiments with correlated χ^2 and χ^2_{Total} per degrees of freedom (dof) for each experiment corresponding to three different HCC, LHCb and HCC+LHCb data sets, when the charm-quark mass is fixed to $m_c = 1.257$ GeV.

In the Table II, we compare the pure impact of the HCC, LHCb and HCC+LHCb data on the fit quality, when the charm-quark mass is fixed to $m_c = 1.257$ GeV. As we can see from numerical results of Table II the best fit quality is corresponding to HCC data.

In Table III, we present NNLO numerical values of 13 free central parameters and their uncertainties for the xu_v , xd_v , sea and gluon distributions at the input scale of $Q_0^2 = 1.9$ GeV²

charm-quark mass is fixed to $m_c = 1.257$ GeV		
Experiment	$\frac{\chi^2_{Total}}{dof}$	fit quality
HCC	1410/1179	1.19
LHCb	2029/1272	1.59
HCC+LHCb	2078/1319	1.57

Table II: Comparison the pure impact of the HCC, LHCb and HCC+LHCb data on the fit quality, when the charm-quark mass is fixed to $m_c = 1.257$ GeV.

for three different HCC, LHCb and HCC+LHCb data sets.

According to the numerical values of Table III and three different fit qualities from Table II, we expect to see dramatically impact of the HCC, LHCb and HCC+LHCb data on the shape of the gluon distribution and some of its ratios.

In Fig. 1, we show the gluon PDFs (two upper), the partial of gluon PDFs (two middle) and the partial ratio of Σ -PDFs over gluon distributions (two lower) as extracted from three different HCC (blue), LHCb (red) and HCC+LHCb (yellow) data sets.

As can be seen from Fig. 1 the best improvement of uncertainty error bands is corresponding to HCC+LHCb data with yellow color, which in turn strictly confirms that the DIS measurements depend on the various phenomenological input data and knowledge of the PDFs. Also, the pure impact of LHCb charm production data in improvement of the gluon distribution and some of its ratios (red color) is better than the pure impact of HCC data (blue color).

Now in the second step we consider the charm-quark mass as an extra free parameter and repeat our previous fit procedures but this time with 14 free parameters to determine both charm-quark mass and pure impact of c -mass on the shape of the proton PDFs and fit quality.

Table IV, shows the experiments with correlated χ^2 and $\frac{\chi^2_{Total}}{dof}$ for each experiment corresponding to three different HCC, LHCb and HCC+LHCb data sets, when the charm-quark mass m_c is taken as an extra pQCD free parameter.

In Table V we compare the pure impact of the HCC, LHCb and HCC+LHCb data sets on the fit-quality, when the charm-quark mass m_c is taken as an extra pQCD free parameter. As we can see from the numerical results of Table V the best fit quality is corresponding to

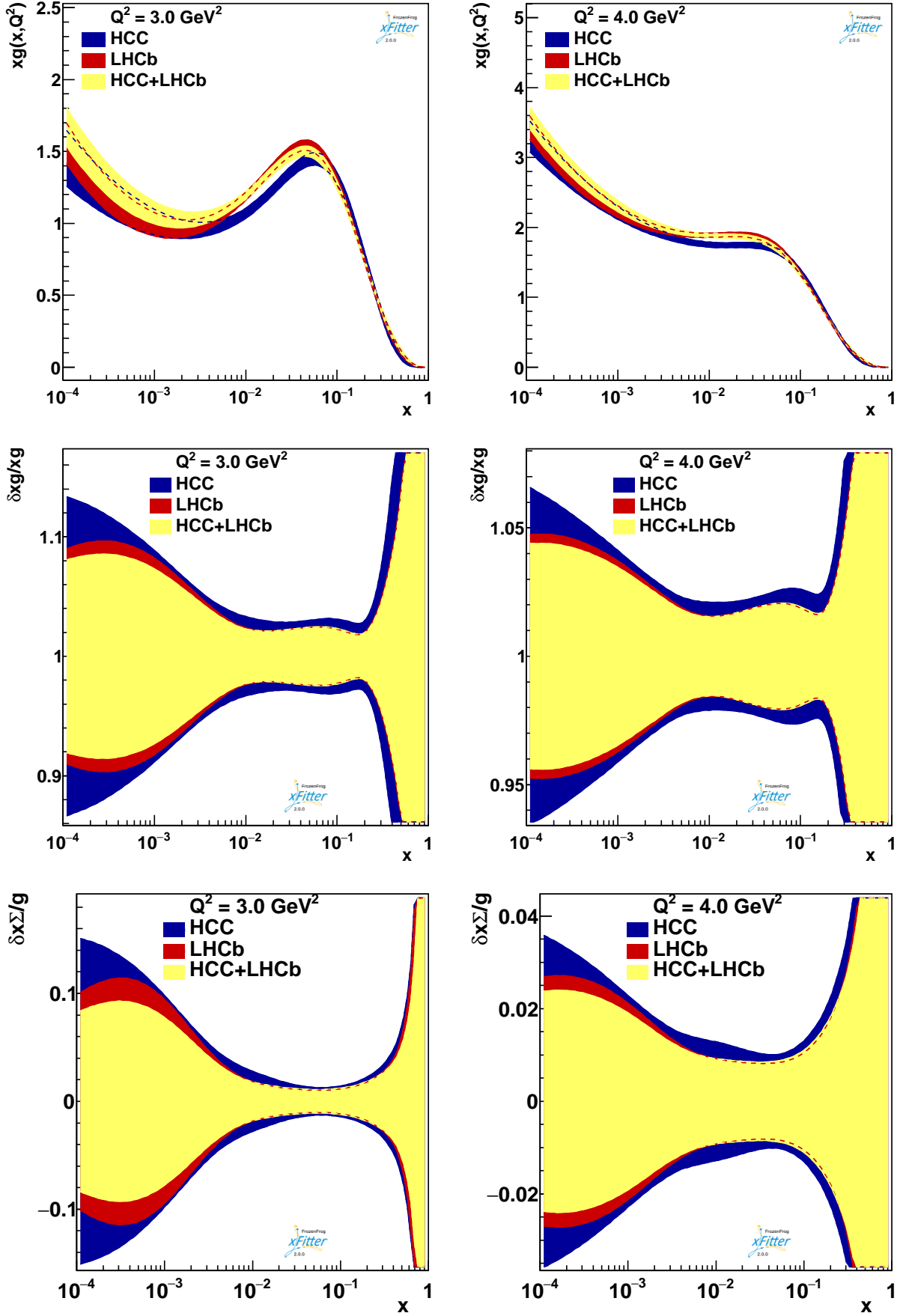


Figure1: The gluon PDFs (two upper), the partial of gluon PDFs (two middle) and the partial ratio of Σ -PDFs over gluon distributions (two lower) as extracted from three different HCC (blue)

charm-quark mass is fixed to $m_c = 1.257$ GeV			
Parameter	HCC	LHCb	HCC+LHCb
B_{u_v}	0.865 ± 0.033	0.831 ± 0.024	0.816 ± 0.025
C_{u_v}	4.392 ± 0.076	4.411 ± 0.087	4.415 ± 0.083
E_{u_v}	9.4 ± 1.3	9.6 ± 1.2	10.2 ± 1.3
B_{d_v}	1.056 ± 0.093	0.978 ± 0.078	0.961 ± 0.079
C_{d_v}	4.47 ± 0.37	4.67 ± 0.39	4.58 ± 0.38
$C_{\bar{U}}$	3.77 ± 0.54	2.35 ± 0.31	2.45 ± 0.32
$A_{\bar{D}}$	0.1801 ± 0.0091	0.1629 ± 0.0072	0.1682 ± 0.0075
$B_{\bar{D}}$	-0.1691 ± 0.0063	-0.1807 ± 0.0056	-0.1757 ± 0.0056
$C_{\bar{D}}$	5.7 ± 1.0	5.69 ± 0.87	5.80 ± 0.90
B_g	0.23 ± 0.13	-0.196 ± 0.026	-0.192 ± 0.027
C_g	4.89 ± 0.77	3.23 ± 0.32	2.99 ± 0.31
A'_g	2.69 ± 0.51	1.75 ± 0.20	1.64 ± 0.19
B'_g	0.101 ± 0.058	-0.161 ± 0.026	-0.157 ± 0.028
$\alpha_s^{\text{NNLO}}(M_Z^2)$	0.118	0.118	0.118
m_c	1.257	1.257	1.257

Table III: The NNLO numerical values of 13 free central parameters and their uncertainties for the xu_v , xd_v , sea and gluon distributions at the input scale of $Q_0^2 = 1.9$ GeV² for three different HCC, LHCb and HCC+LHCb data sets.

the HCC data set.

In Fig. 2, we show the gluon PDFs (two upper), the partial of gluon PDFs (two middle) and the partial ratio of Σ -PDFs over gluon distributions (two lower) as extracted from three different HCC (blue), LHCb (red) and HCC+LHCb (yellow) data sets.

It is clear from the Fig. 2 that the best improvement of uncertainty error bands is corresponding to HCC+LHCb data with green color. Also, the pure impact of LHCb charm production data in improvement of the gluon distribution and some of its ratios (yellow color) is significantly better than the pure impact of HCC data (blue color).

As one can find from the Fig. 2 (top 2 plots), the blue lines (HCC) clearly are separated from the yellow lines (LHCb). This issue physically means that, the actual charm-quark

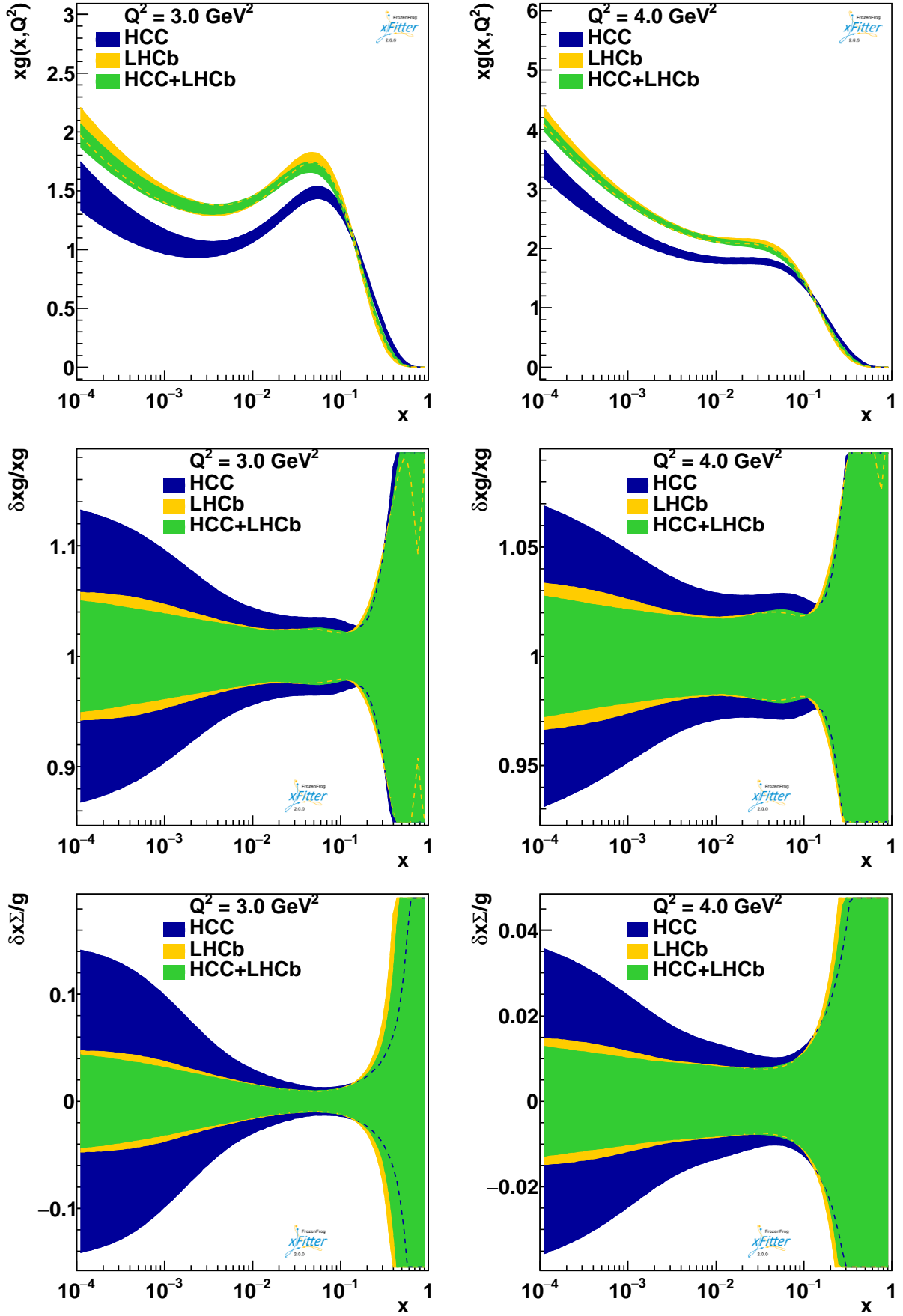


Figure 2: The gluon PDFs (two upper), the partial of gluon PDFs (two middle) and the partial ratio of Σ -PDFs over gluon distributions (two lower) as extracted from three different HCC (blue)

Scheme	m_c is taken as an extra pQCD free parameter		
Experiment	HCC	LHCb	HCC+LHCb
HC CC e^+p [27]	55 / 39	57 / 39	58 / 39
HC CC e^-p [27]	51 / 42	51 / 42	51 / 42
HC NC e^-p [27]	218 / 159	223 / 159	225 / 159
HC NC e^+p 460 [27]	213 / 204	209 / 204	208 / 204
HC NC e^+p 575 [27]	213 / 254	211 / 254	210 / 254
HC NC e^+p 820 [27]	63 / 70	63 / 70	63 / 70
HC NC e^+p 920 [27]	425 / 377	418 / 377	420 / 377
HCC [1]	43 / 47	-	58 / 47
LHCb 7TeV Dzero [2]	-	108 / 38	128 / 38
LHCb 7TeV Dch [2]	-	69 / 37	73 / 37
LHCb 7TeV Dstar [2]	-	50 / 31	54 / 31
LHCb 7TeV Ds [2]	-	30 / 28	28 / 28
LHCb 7TeV Lambdac [2]	-	7.0 / 6	6.3 / 6
Correlated χ^2	157	215	261
$\frac{\chi^2_{Total}}{dof}$	$\frac{1438}{1178}$	$\frac{1710}{1271}$	$\frac{1844}{1318}$

Table IV: Experiments with correlated χ^2 and $\frac{\chi^2_{Total}}{dof}$ for each experiment corresponding to three different HCC, LHCb and HCC+LHCb data sets, when the charm-quark mass m_c is taken as an extra pQCD free parameter.

pole mass m_c^{pole} increases at higher energies in the scattering process.

According to the absolute relative change of χ^2 function which is defined by $|\frac{\chi^2_{\text{final}} - \chi^2_{\text{initial}}}{\chi^2_{\text{initial}}}|$, we may conclude from numerical results of the Tables II and V:

- Relative improvement in the quality of the fit corresponding to HCC data is $|\frac{1.22-1.19}{1.19}| \sim 2.5$ %, without and with the charm-quark mass m_c is taken as an extra pQCD free parameter.
- Relative improvement in the quality of the fit corresponding to LHCb data is $|\frac{1.34-1.59}{1.59}| \sim 15.7$ %, with and without the charm-quark mass m_c is taken as an extra pQCD free parameter.

charm-quark mass is taken as an extra free parameter		
Experiment	$\frac{\chi^2_{Total}}{dof}$	fit quality
HCC	1438/1178	1.22
LHCb	1710/1271	1.34
HCC+LHCb	1844/1318	1.40

Table V: Comparison the pure impact of the HCC, LHCb and HCC+LHCb data on the fit quality, when the charm-quark mass m_c is taken as an extra pQCD free parameter.

- Relative improvement in the quality of the fit corresponding to HCC+LHCb data is $|\frac{1.40-1.57}{1.57}| \sim 10.8 \%$, with and without the charm-quark mass m_c is taken as an extra pQCD free parameter.

Since the χ^2 function is a measure of the agreement between data and theory models, we led to this fact that: deep inelastic $e^\pm p$ scattering measurements depend on the various phenomenological input data. On the other hand, dramatically improvement of the error bands of the gluon content of the proton corresponding to LHCb data, strictly confirms these results.

Determination of the 14 free fit parameters, including 13 central proton PDF parameters and charm-quark mass m_c as an extra pQCD free parameter are presented in Table VI.

As we expected, the best uncertainty improvement from the central value of c -quark mass is $m_c = 1.655 \pm 0.022$, corresponding to HCC+LHCb data sets.

The comparison of these results with the measurements from the PDG world average [46] shows a very good agreement with the expected charm-quark mass.

The pure impact of c -mass on gluon distribution and consistency between pQCD theory predictions and the phenomenology of experimental data in determination of the charm-quark pole mass m_c^{pole} at the NNLO corrections in three separate panels, include of pulls, $\frac{\text{Theory+Shifts}}{\text{Data}}$ and $\frac{\text{Theory}}{\text{Data}}$ corresponding to HCC and LHCb data sets are shown in Figs. 3 and 4.

charm-quark mass is taken as an extra free parameter			
Parameter	HCC	LHCb	HCC+LHCb
B_{uv}	0.865 ± 0.032	0.860 ± 0.026	0.834 ± 0.024
C_{uv}	4.387 ± 0.079	4.39 ± 0.11	4.45 ± 0.10
E_{uv}	9.3 ± 1.3	8.4 ± 1.3	9.6 ± 1.3
B_{dv}	1.050 ± 0.091	1.012 ± 0.082	0.977 ± 0.079
C_{dv}	4.47 ± 0.37	4.79 ± 0.39	4.72 ± 0.39
$C_{\bar{U}}$	3.59 ± 0.56	2.35 ± 0.30	2.21 ± 0.28
$A_{\bar{D}}$	0.1834 ± 0.0096	0.1936 ± 0.0078	0.1897 ± 0.0074
$B_{\bar{D}}$	-0.1669 ± 0.0066	-0.1589 ± 0.0049	-0.1601 ± 0.0046
$C_{\bar{D}}$	5.7 ± 1.0	5.36 ± 0.86	5.49 ± 0.89
B_g	0.24 ± 0.14	0.212 ± 0.096	0.151 ± 0.090
C_g	5.27 ± 0.87	8.07 ± 0.62	6.57 ± 0.62
A'_g	2.95 ± 0.60	5.77 ± 0.86	3.77 ± 0.60
B'_g	0.112 ± 0.063	0.162 ± 0.057	0.097 ± 0.052
$\alpha_s^{\text{NNLO}}(M_Z^2)$	0.118	0.118	0.118
m_c	1.331 ± 0.058	1.760 ± 0.028	1.655 ± 0.022

Table VI: The NNLO numerical values of 14 free fit parameters, including 13 central proton PDF parameters and charm-quark mass m_c as an extra pQCD free parameter for three different HCC, LHCb and HCC+LHCb data sets.

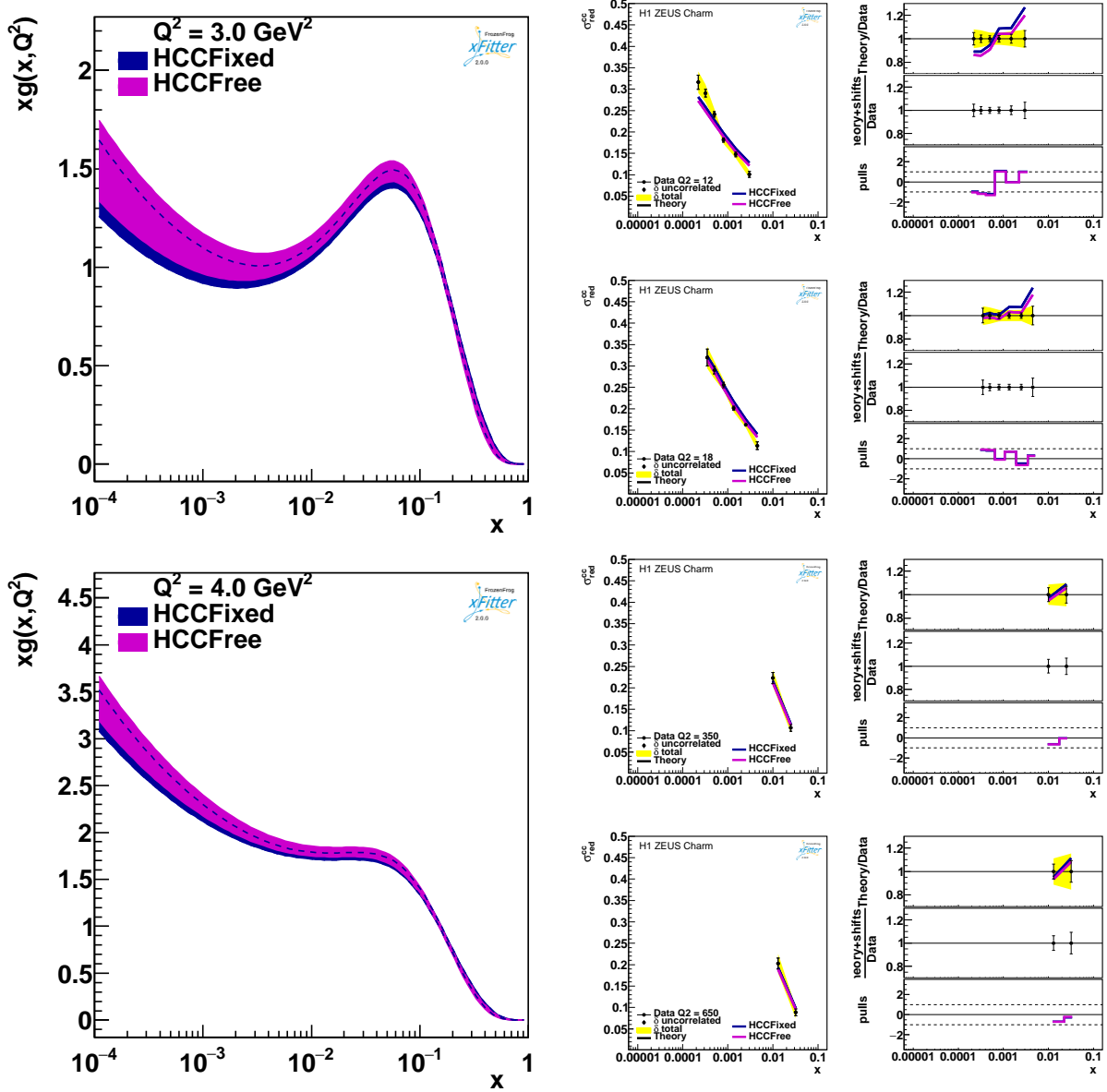
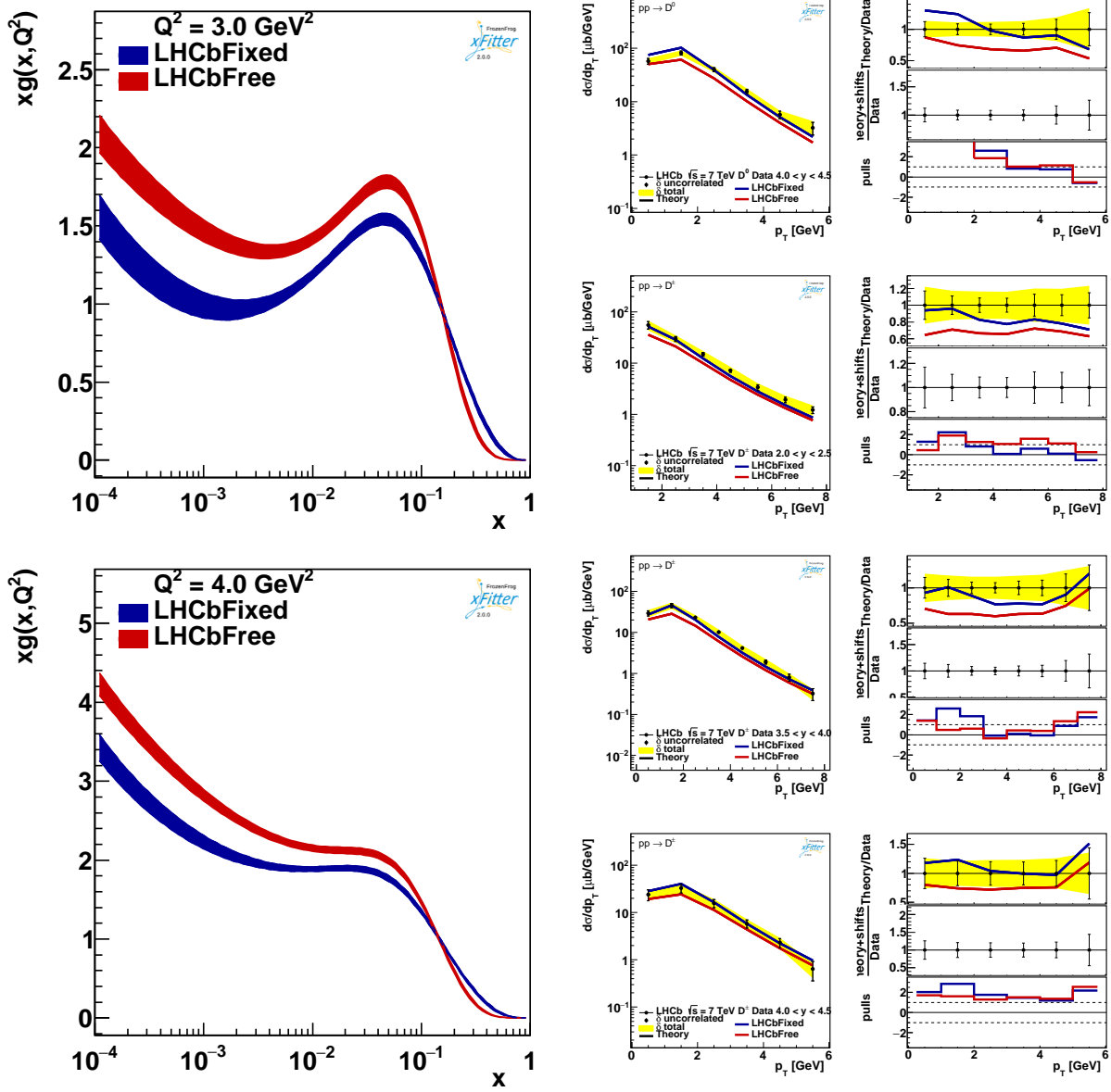


Figure 3: The pure impact of c -mass on gluon distribution and consistency between pQCD theory predictions and the phenomenology of experimental data in determination of the charm-quark pole mass m_c^{pole} at the NNLO corrections in three separate panels, include of pulls, $\frac{\text{Theory}+\text{Shifts}}{\text{Data}}$ and $\frac{\text{Theory}}{\text{Data}}$ corresponding to HCC data set.



VI. SUMMARY

Using three deferent HCC, LHCb and HCC+LHCb data sets, we have simultaneously determined proton PDFs and charm-quark pole mass m_c^{pole} at the NNLO corrections.

We have studied the pure impact of the three deferent HCC, LHCb and HCC+LHCb data sets and also pure contribution of charm-quark mass m_c on the uncertainty bands of proton PDFs and fit-quality in two separate steps with following results:

- The best improvement of uncertainty error bands is corresponding to HCC+LHCb data, which strictly confirms that the deep inelastic $e^\pm p$ scattering measurements depend on the various phenomenological input data and knowledge of the proton PDFs.
- Because of correlation between proton PDFs and charm-quark pole mass m_c^{pole} as an extra free parameter of the pQCD Lagrangian, the gluon content of the proton is dramatically sensitive to c -mass.
- We have shown that, the actual charm-quark pole mass m_c^{pole} increases at higher energies in the deep inelastic $e^\pm p$ scattering measurements scattering process.
- The best relative improvement in the quality of the fit is corresponding to LHCb data up to 15.7 %, with and without the charm-quark mass m_c is taken as an extra pQCD free parameter.
- The best uncertainty improvement from the central value of c -quark mass is $m_c = 1.655 \pm 0.022$, corresponding to HCC+LHCb data sets, which emphasizes once again, the DIS measurements depend strictly on the various phenomenological input data sets.

In this NNLO pQCD analysis, we presented the central role of charm-quark pole mass m_c^{pole} in the improvement of uncertainty band of gluon distribution and QCD fit-quality, when it is considered as an extra free parameter of the pQCD Lagrangian.

Standard LHAPDF library files of all fit processes are available and can be obtained via e-mail from the authors.

VII. ACKNOWLEDGMENTS

We gratefully acknowledge Prof. V. Radescu for guidance and useful discussions about PDFs and xFitter. We are grateful to Prof. M. Botje for providing the QCDNUM package as a very fast QCD evolution program. We are also grateful to Prof. F. Olness for developing valuable heavy-flavor schemes as implemented in the xFitter package. We would like to thanks Dr. Francesco Giuli, Dr. Ivan Novikov, Dr. Oleksandr Zenaiev and Dr. Sasha Glazov from xFitter developer group for guidance and technical support. This work is related to the “Special Support Program for the Promotion of Scientific Authority” in Ferdowsi University of Mashhad.

-
- [1] H. Abramowicz *et al.* [H1 and ZEUS], Eur. Phys. J. C **78**, no.6, 473 (2018) [arXiv:1804.01019 [hep-ex]].
 - [2] R. Aaij *et al.* [LHCb Collaboration], Nucl. Phys. B **871**, 1 (2013) [arXiv:1302.2864 [hep-ex]].
 - [3] S. Alekhin, J. Blöchl, K. Daum, K. Lipka and S. Moch, Phys. Lett. B **720**, 172 (2013) [arXiv:1212.2355 [hep-ph]].
 - [4] J. Gao, M. Guzzi and P. M. Nadolsky, Eur. Phys. J. C **73**, no. 8, 2541 (2013) [arXiv:1304.3494 [hep-ph]].
 - [5] W. K. Tung, H. L. Lai, A. Belyaev, J. Pumplin, D. Stump and C.-P. Yuan, JHEP **0702**, 053 (2007) [hep-ph/0611254].
 - [6] F. D. Aaron *et al.* [H1 and ZEUS Collaborations], JHEP **1001**, 109 (2010) [arXiv:0911.0884 [hep-ex]].
 - [7] J. Blumlein, Prog. Part. Nucl. Phys. **69**, 28 (2013) [arXiv:1208.6087 [hep-ph]].
 - [8] O. Zenaiev, Eur. Phys. J. C **77**, no. 3, 151 (2017) [arXiv:1612.02371 [hep-ex]].
 - [9] O. Zenaiev *et al.* [PROSA Collaboration], Eur. Phys. J. C **75**, no. 8, 396 (2015) [arXiv:1503.04581 [hep-ph]].
 - [10] R. Aaij *et al.* [LHCb Collaboration], JHEP **1308**, 117 (2013) [arXiv:1306.3663 [hep-ex]].
 - [11] R. Aaij *et al.* [LHCb Collaboration], JHEP **1603**, 159 (2016) Erratum: [JHEP **1609**, 013 (2016)] Erratum: [JHEP **1705**, 074 (2017)] [arXiv:1510.01707 [hep-ex]].
 - [12] R. Aaij *et al.* [LHCb Collaboration], JHEP **1706**, 147 (2017) [arXiv:1610.02230 [hep-ex]].
 - [13] A. A. Alves, Jr. *et al.* [LHCb Collaboration], JINST **3**, S08005 (2008).
 - [14] M. Adinolfi *et al.* [LHCb RICH Group], Eur. Phys. J. C **73**, 2431 (2013) [arXiv:1211.6759 [physics.ins-det]].
 - [15] A. Vafaei and A. N. Khorramian, Nucl. Phys. B **921**, 472 (2017) [arXiv:1709.08346 [hep-ph]].
 - [16] S. Alekhin, K. Daum, K. Lipka and S. Moch, Phys. Lett. B **718**, 550 (2012) [arXiv:1209.0436 [hep-ph]].
 - [17] S. Alekhin, J. Blöchl, S. Moch and R. Placakyte, Phys. Rev. D **96**, no. 1, 014011 (2017) [arXiv:1701.05838 [hep-ph]].
 - [18] A. L. Kataev and V. S. Molokoedov, arXiv:1809.04395 [hep-ph].
 - [19] P. Marquard, A. V. Smirnov, V. A. Smirnov and M. Steinhauser, PoS RADCOR **2015**, 094

- (2016) [arXiv:1601.03748 [hep-ph]].
- [20] P. Marquard, A. V. Smirnov, V. A. Smirnov and M. Steinhauser, Phys. Rev. Lett. **114**, no. 14, 142002 (2015) [arXiv:1502.01030 [hep-ph]].
 - [21] M. Beneke, Phys. Lett. B **434**, 115 (1998) [hep-ph/9804241].
 - [22] S. J. Brodsky, arXiv:1709.01191 [hep-ph].
 - [23] S. J. Brodsky, Russ. Phys. J. **60** (2017) no.3, 399.
 - [24] Z. H. Weng, Adv. Math. Phys. **2017**, 9876464 (2017) [arXiv:1704.02240 [physics.gen-ph]].
 - [25] L. Bravina, A. Di Giacomo, Y. Foka and S. Kabana, EPJ Web Conf. **70**, 00019 (2014).
 - [26] A. Vafaei and K. Javidan, Mod. Phys. Lett. A **35**, no.30, 2050253 (2020) [arXiv:1909.00796 [hep-ph]].
 - [27] H. Abramowicz *et al.* [H1 and ZEUS Collaborations], Eur. Phys. J. C **75**, no. 12, 580 (2015) [arXiv:1506.06042 [hep-ex]].
 - [28] H. L. Lai, M. Guzzi, J. Huston, Z. Li, P. M. Nadolsky, J. Pumplin and C.-P. Yuan, Phys. Rev. D **82**, 074024 (2010) [arXiv:1007.2241 [hep-ph]].
 - [29] R. D. Ball *et al.* [NNPDF Collaboration], Nucl. Phys. B **809**, 1 (2009) Erratum: [Nucl. Phys. B **816**, 293 (2009)] [arXiv:0808.1231 [hep-ph]].
 - [30] A. Mironov and A. Morozov, JHEP **1004**, 040 (2010) [arXiv:0910.5670 [hep-th]].
 - [31] J. C. Collins, Phys. Rev. D **58**, 094002 (1998) [hep-ph/9806259].
 - [32] A. D. Martin, W. J. Stirling and R. S. Thorne, Phys. Lett. B **636**, 259 (2006) [hep-ph/0603143].
 - [33] S. Forte, E. Laenen, P. Nason and J. Rojo, Nucl. Phys. B **834**, 116 (2010) [arXiv:1001.2312 [hep-ph]].
 - [34] A. D. Martin, W. J. Stirling, R. S. Thorne and G. Watt, Eur. Phys. J. C **63**, 189 (2009) [arXiv:0901.0002 [hep-ph]].
 - [35] R. S. Thorne, Phys. Rev. D **73**, 054019 (2006) [hep-ph/0601245].
 - [36] R. S. Thorne, Phys. Rev. D **86**, 074017 (2012) [arXiv:1201.6180 [hep-ph]].
 - [37] xFitter, An open source QCD fit framework. <http://xFitter.org> [xFitter.org] [arXiv:1410.4412 [hep-ph]].
 - [38] A. Vafaei, K. Javidan and A. Shokouhi, [arXiv:1906.07390 [hep-ph]].
 - [39] A. Vafaei and A. Shokouhi, [arXiv:1904.04285 [hep-ph]].
 - [40] A. Shokouhi and A. Vafaei, Nucl. Part. Phys. Proc. **300-302**, 35-39 (2018)
 - [41] A. Vafaei, Nucl. Part. Phys. Proc. **300-302**, 30-34 (2018)

- [42] A. Vafaei and A. Khorramian, Nucl. Part. Phys. Proc. **282-284**, 32 (2017).
- [43] A. Vafaei, A. Khorramian, S. Rostami and A. Aleedaneshvar, Nucl. Part. Phys. Proc. **270-272**, 27 (2016).
- [44] M. Botje, Comput. Phys. Commun. **182**, 490 (2011) [arXiv:1005.1481 [hep-ph]].
- [45] V. N. Gribov and L. N. Lipatov, Sov. J. Nucl. Phys. **15**, 438 (1972) [Yad. Fiz. **15**, 781 (1972)];
L. N. Lipatov, Sov. J. Nucl. Phys. **20**, 94 (1975) [Yad. Fiz. **20**, 181 (1974)];
Y. L. Dokshitzer, Sov. Phys. JETP **46**, 641 (1977) [Zh. Eksp. Teor. Fiz. **73**, 1216 (1977)];
G. Altarelli and G. Parisi, Nucl. Phys. B **126**, 298 (1977).
- [46] K. A. Olive *et al.* [Particle Data Group], Chin. Phys. C **38**, 090001 (2014).